Fortschritte der Physik

Fortschritte der Physik
Progress of Physics
www.fp-journal.org

RESEARCH ARTICLE OPEN ACCESS

Quasinormal Modes for Coherent Quantum Black Holes

Tommaso Antonelli[1] | Andrea Giusti[2,3] | Roberto Casadio[2,3] | Lavinia Heisenberg[4]

[1]Department of Physics and Astronomy, University of Sussex, Brighton, United Kingdom | [2]DIFA & AM[2], Università di Bologna, Bologna, Italy | [3]I.N.F.N., Sezione di Bologna, I.S. FLAG, Bologna, Italy | [4]Institute for Theoretical Physics, Heidelberg University, Heidelberg, Germany

Correspondence: Andrea Giusti (andrea.giusti9@unibo.it)

Received: 28 December 2025 | **Revised:** 8 March 2026 | **Accepted:** 10 March 2026

ABSTRACT

Coherent quantum black holes are quantum geometries obtained by means of a mean-field-like approach to the gravitational interaction. This procedure attenuates the classical spacetime singularities of general relativity by replacing them with integrable singularities in the quantum-corrected geometry. After discussing some relevant observables for a novel geometry for spherically symmetric black holes, we investigate the quasinormal modes spectrum of scalar, electromagnetic, and gravitational fields for the proposed model. The results indicate potential deviations from general relativity, the magnitude of which is gauged by the value of the ultraviolet regulator of the model (physically identifiable as a matter core). Observations of the ringdown phase in black hole mergers could help detect such deviations.

1 | Introduction

Coherent quantum black holes are emerging quantum geometries for which the metric tensor is obtained, following a mean-field-like approach to the gravitational interaction, which is expected to hold also in the strong-coupling regime.

Let us consider a static spherically symmetric line element

$$ds^2 = -f(r)\,dt^2 + \frac{dr^2}{f(r)} + r^2\,d\Omega^2\,, \qquad f = 1 + 2\,V(r)\,, \tag{1}$$

where $d\Omega^2$ denotes the line element on the 2-sphere, r is the areal radius, and we shall refer to $V = V(r)$ as potential function, although no weak-field approximation is involved in the construction.[1]

If we consider a classical reference geometry (from general relativity) given in terms of the potential $V = V_{\rm c}(r)$, then one can think of this geometry as the expectation value of a metric tensor operator $\widehat{g}_{ab}$ over a suitable quantum state $|g\rangle$, that is

$$\langle g|\widehat{V}|g\rangle = V_{\rm c}(r)\,. \tag{2}$$

The underlying idea of the coherent state approach [1] is to describe $\widehat{V}$ as a free massless scalar field which is meant to represent the non-perturbative collective behaviour of the only gravitational degree of freedom required to reproduce the solution $V_{\rm c}$ from the quantitation of the Einstein theory. Hence, within this approach, a certain classical configuration $V = V_{\rm c}(r)$ can be realised if there exists a coherent state $|g\rangle$ of the field $\widehat{V}$ such that Equation (2) holds. The total occupation number N enters the normalisation of the coherent state $|g\rangle$ and measures the distance of $|g\rangle$ from the vacuum $|0\rangle$, the latter being understood as the state devoid of any gravitational and matter excitation [1].

Taking the Schwarzschild metric with

$$V_{\rm c} = -\frac{M}{r} \tag{3}$$

as the reference classical geometry and characterising the associated coherent state in momentum space, one finds [1]

$$N = 4\,M^2 \int_0^\infty \frac{dk}{k}\,, \tag{4}$$

which diverges both in the ultraviolet (UV) and in the infrared (IR) regimes. This means that the exact Schwarzschild black hole cannot be realised within the coherent state approach, and a regularisation is required in order to find a coherent state that closely (yet, not exactly) reproduces the Schwarzschild metric. As discussed in ref. [2], this can be achieved by introducing an IR cut-off accounting for the finite lifetime of a black hole, say $\tau \sim R_\infty \equiv k_{\rm IR}^{-1}$, and a Gaussian regulator related to a quantum core of finite size $R_{\rm s} \equiv k_{\rm UV}^{-1}$. This yields

$$N = 4\,M^2 \int_{R_\infty^{-1}}^{\infty} \frac{e^{-(R_{\rm s}\,k)^2/2}}{k}\,dk \simeq 4\,M^2\,\log\left(\frac{R_\infty}{R_{\rm s}}\right), \tag{5}$$

under the assumption that $R_{\rm s} \ll R_\infty$. This regularisation, when implemented at the level of the potential, yields a quantum-corrected Schwarzschild geometry defined by the quantum potential [2]

$$V_{\rm q} = -\frac{M}{r}\,{\rm erf}\left(\frac{r}{R_{\rm s}}\right), \tag{6}$$

where ${\rm erf}(z)$ denotes the error function. Clearly, Equation (6) tells us that the size of the quantum core $R_{\rm s}$ gauges the strength of the corrections to the classical Schwarzschild potential, which is (formally) obtained for $R_{\rm s} \to 0^+$.

A similar analysis has been performed for electrically charged black holes [3], where the regularisation of the UV divergence was carried out by means of a sharp UV cut-off as in ref. [1] for the electrically neutral case. The problem with this regularisation is that it introduces (spurious) osculations in the quantum potential, due to the fact that the error function in Equation (6) is replaced by a sine-integral function. This feature is removed by the smoother regularisation adopted in ref. [2]. Notably, the Gaussian regulator used in ref. [2] does not affect the main interior features of the quantum core originally derived in ref. [1]. Specifically, our quantum-corrected black hole contains an integrable singularity at its center, as we shall discuss in Section 2.

Quasinormal modes are the characteristic oscillations of perturbations propagating on a black hole background geometry. If we denote by ψ the propagating physical degree of freedom associated to a given perturbed field on a metric of the form (1), one can express its time dependence as

$$\psi \sim e^{-i\,\omega\,t}, \tag{7}$$

with ω being the quasinormal mode frequency of the black hole. The peculiarity of perturbation theory on a black hole background is that the system is dissipative (due to the presence of an event horizon) and the frequencies ω for modes that are purely outgoing at infinity are therefore complex,

$$\omega = \omega_{\rm R} + i\,\omega_{\rm I}, \qquad \omega_{\rm I} < 0, \tag{8}$$

with the imaginary part yielding the timescale of decay for the mode. (Excellent reviews of black hole quasinormal modes are, for instance, refs. [4–6].)

For the purposes of this work, we will focus solely on perturbations outside the event horizon, since this is the most relevant region of spacetime for astrophysical observations, and we will consider perturbations of three different types of fields: scalar, electromagnetic, and gravitational. The scalar field represents a simple toy model that contains the relevant features for a stability analysis of the solution, without the mathematical complications of gauge fields. The electromagnetic and gravitational fields are of course more interesting from a phenomenological perspective.

This work is organised as follows: in Section 2, we review the quantum-corrected Schwarzschild black hole obtained within the coherent state approach in ref. [2]; in Section 3, we estimate the quasinormal mode frequencies for this geometry via the semi-analytical WKB procedure proposed in Ref. [6]; lastly, a discussion and outlook on future research is presented in Section 4.

2 | Quantum-Corrected Schwarzschild Geometry

Let us consider the line element in Equation (1) with $f = f_{\rm q} = 1 + 2\,V_{\rm q}(r)$ and the quantum potential $V_{\rm q}$ defined in Equation (6). Recalling that the line element of a static spherically symmetric spacetime, with vanishing anomalous redshift, can be parametrised in terms of the Misner–Sharp–Hernandez mass $m = m(r)$ as (see, e.g., ref. [7])

$$f_{\rm q} = 1 - \frac{2\,m(r)}{r}, \tag{9}$$

one can easily infer that

$$m = -r\,V_{\rm q}(r) = M\,{\rm erf}\left(\frac{r}{R_{\rm s}}\right). \tag{10}$$

Taking advantage of the discussion in ref. [8] for general static spherically symmetric spacetimes, one can easily compute the Kretschmann scalar $\mathcal{K} = R^{\mu\nu\alpha\beta}\,R_{\mu\nu\alpha\beta}$ and the effective energy–momentum tensor for our quantum-corrected Schwarzschild geometry. Interestingly, since

$$m = \frac{2\,M\,r}{\sqrt{\pi}\,R_{\rm s}} + \mathcal{O}\left[\left(\frac{r}{R_{\rm s}}\right)^3\right], \tag{11}$$

for $r \to 0^+$, it is easy to see that

$$\mathcal{K} = \mathcal{O}\left(\frac{1}{r^4}\right), \tag{12}$$

$$\rho = -p_r = \frac{m'(r)}{4\,\pi\,r^2} = \mathcal{O}\left(\frac{1}{r^2}\right), \tag{13}$$

$$p_\theta = p_\phi = \frac{m''(r)}{8\,\pi\,r} = \mathcal{O}(1), \tag{14}$$

for $r \to 0^+$, where ρ, p_r, p_θ, and p_ϕ denote the effective energy density and pressures associated with the quantum-corrected metric.

From Equations (12)–(14), one can easily conclude that the spacetime still contains a curvature singularity at $r = 0$, but the divergence of $\mathcal{K}$ is much milder than Schwarzschild's $\mathcal{K}_{\rm Sch} = \mathcal{O}(1/r^6)$. Furthermore, although the effective energy–momentum tensor has divergences at $r = 0$, the volume integrals of the effective energy density and pressures are finite in any neighbourhood

of $r = 0$, that is,

$$\left|4\,\pi \int_0^{\epsilon} \rho(\bar{r})\,\bar{r}^2\,d\bar{r}\right| < \infty$$

$$\text{and} \qquad \left|4\,\pi \int_0^{\epsilon} p_i(\bar{r})\,\bar{r}^2\,d\bar{r}\right| < \infty\,, \quad \forall \epsilon > 0\,, \tag{15}$$

where $i = (r, \theta, \phi)$. In other words, we find that our quantum corrected geometry has an integrable singularity at $r = 0$ (see ref. [9] for more details).

The existence of an integrable singularity at the centre of a coherent quantum black hole was already pointed out in refs. [1, 3], although with a different regularisation procedure. Here, we have shown that replacing the sharp UV cut-off with a Gaussian regulator does not affect the behaviour of the quantum corrected metric near $r = 0$.

For a spacetime metric (1), the location of horizons is given by the solutions of the equation

$$f_{\rm q}(r_{\rm H}) = 1 + 2V_{\rm q}(r_{\rm H}) = 0\,, \tag{16}$$

equivalent to $r_{\rm H} = 2\,m(r_{\rm H})$. Then, it is easy to see that Equation (16) admits an event horizon if and only if

$$R_{\rm s} < \frac{4\,M}{\sqrt{\pi}} = \frac{2\,R_{\rm Sch}}{\sqrt{\pi}} \approx 1.13\,R_{\rm Sch}\,, \tag{17}$$

where $R_{\rm Sch} = 2\,M$ is the Schwarzschild radius. If we further require the quantum core to be hidden inside the actual event horizon at $r_{\rm H}$, that is, $R_{\rm s} < r_{\rm H}$, we have the additional restriction on the size of the core

$$R_{\rm s} < {\rm erf}(1)\,R_{\rm Sch} \approx 0.84\,R_{\rm Sch}\,. \tag{18}$$

The above bound implies that a core of size $R_{\rm s} = R_{\rm Sch}$ could be considered as a kind of black hole *mimicker* (like the *gravastars* [10]).

As discussed in ref. [11], several physical observable can be computed in order to investigate deviations from general relativity in the context of coherent quantum geometries. For instance, a rather straightforward problem is to compute the location of the photon ring R_γ, defined as the solution to the equation [11]

$$R_\gamma\,f_{\rm q}'(R_\gamma) - 2\,f_{\rm q}(R_\gamma) = 0\,, \tag{19}$$

which ultimately represents the lowest bound for stable orbits.

Another interesting observable is the critical impact parameter for massless particles $b_{\rm c}$, which is defined as [11]

$$b_{\rm c} = \frac{R_\gamma}{\sqrt{f_{\rm q}(R_\gamma)}}\,, \tag{20}$$

and represents the minimal ratio of the angular momentum over the energy of the massless particle below which the particle falls into the black hole.

In Figure 1, we display the magnitude of the deviations of $r_{\rm H}$, R_γ, and $b_{\rm c}$ from the corresponding values for the Schwarzschild solution (for which $r_{\rm H} = R_{\rm Sch}$, $R_\gamma = 3\,R_{\rm Sch}/2$ and $b_{\rm c} = 3\sqrt{3}R_{\rm Sch}/2$) as we vary the size of the quantum core $R_{\rm s}$.

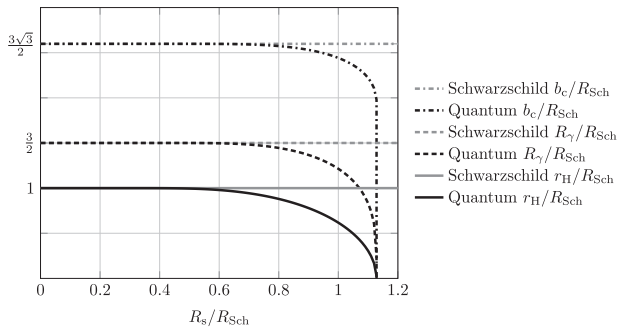

FIGURE 1 | Values of $r_{\rm H}$, R_γ and $b_{\rm c}$ in units of $R_{\rm Sch}$ as a function of the size of the quantum core $R_{\rm s}$.

3 | Quasinormal Modes

Quasinormal modes of a static spherical symmetric black hole, for scalar perturbations, can be computed by considering a scalar field Φ satisfying the Klein–Gordon equation

$$\left(\Box - m^2\right)\Phi = 0\,. \tag{21}$$

It is convenient to decompose the scalar field in Fourier modes and spherical harmonics $Y_\ell^m = Y_\ell^m(\theta, \varphi)$,

$$\Phi = \int d\omega \sum_{\ell m} e^{-i\,\omega\,t}\,\Phi_{\omega \ell m}(r, \theta, \varphi)\,. \tag{22}$$

where [2]

$$\Phi_{\omega \ell m} = F_{\omega \ell m}(r)\,Y_\ell^m(\theta, \varphi)\,, \tag{23}$$

with $\ell = 0, 1, \ldots$ and $m = -\ell, \ldots, \ell$ as usual. Plugging this ansatz into Equation (21), and adopting the field redefinition

$$\psi_0(r) \equiv r\,F_{\omega \ell m}(r)\,, \tag{24}$$

turns Equation (21) into

$$\frac{d^2\psi_0}{dr_*^2} + \left[\omega^2 - V_0(r)\right]\psi_0 = 0\,, \tag{25}$$

where r_* denotes the tortoise coordinate, defined by the condition $dr_* = dr/f(r)$, and

$$V_0 = f(r)\left[\frac{\ell(\ell+1)}{r^2} + \frac{f'(r)}{r} + m^2\right]. \tag{26}$$

More general perturbations ψ_j can be shown to satisfy similar Schrödinger-like equations

$$\frac{d^2\psi_j}{dr_*^2} + \left[\omega^2 - V_j(r)\right]\psi_j = 0\,, \tag{27}$$

where the potential $V_i = V_j(r)$ is uniquely defined for each propagating degree of freedom ψ_j.

Quasinormal modes are solutions of Equation (27) in the region outside the event horizon with appropriate boundary conditions

for their asymptotic expansions. Assuming that the potential V_j is finite for $r \to r_{\rm H}^+$ and $r \to \infty$, the function ψ_j behaves as

$$\psi_j(r_*) \sim \begin{cases} Z_{\rm H}^{(\rm out)}\, e^{-i\,k_{\rm H}\,r_*} + Z_{\rm H}^{(\rm in)}\, e^{+i\,k_{\rm H}\,r_*} & \text{for} \quad r \to r_{\rm H}^+ \\ Z_{\infty}^{(\rm out)}\, e^{+i\,k_{\infty}\,r_*} + Z_{\infty}^{(\rm in)}\, e^{-i\,k_{\infty}\,r_*} & \text{for} \quad r \to \infty\,, \end{cases} \tag{28}$$

where

$$k_{\rm H}^2 = \omega^2 - \lim_{r\to r_{\rm H}^+} V_j(r)\,, \qquad {\rm Re}(k_{\rm H}) > 0 \tag{29}$$

and

$$k_{\infty}^2 = \omega^2 - \lim_{r\to \infty} V_j(r)\,, \qquad {\rm Re}(k_{\infty}) > 0\,. \tag{30}$$

The coefficients $Z_{\rm H}^{(\rm out/in)}$ represent the amplitudes of outgoing and ingoing modes at the horizon, respectively. Similarly, $Z_{\infty}^{(\rm out/in)}$ are the amplitudes of modes escaping towards or falling from infinity. Since no information can exit the horizon[3] and we are only interested in perturbations generated near the black hole, we assume

$$Z_{\rm H}^{(\rm in)} = Z_{\infty}^{(\rm in)} = 0\,. \tag{31}$$

This completely characterises the quasinormal mode frequencies ω, which are found to be quantised.

For a scalar field (spin $j = 0$) with mass m, minimally coupled to gravity, the potential V_0 is given in Equation (26). For the electromagnetic field (spin $j = 1$), minimally coupled to gravity, we have two propagating degrees of freedom (even and odd), which share the same potential [12]

$$V_1(r) = f(r)\,\frac{\ell(\ell+1)}{r^2}\,. \tag{32}$$

Lastly, the gravitational perturbations (spin $j = 2$) have two propagating degrees of freedom governed by different potentials, namely

$$V_2^{(\rm o)}(r) = f(r)\left[\frac{\ell(\ell+1)}{r^2} - \frac{2\,(1-f(r))}{r^2} - \frac{f'(r)}{r}\right], \tag{33}$$

for odd perturbations, and

$$\begin{aligned} V_2^{(\rm e)}(r) = {} & \frac{f(r)}{r^2[\ell(\ell+1) - 2f(r) + rf'(r)]^2} \\ & \times \Big\{ 2f(r)^2\Big[2\ell(\ell+1) + r^3 f'''(r)\Big] \\ & + \Big[r^2 f'(r)^2 - r^3 f'(r) f''(r) + \ell(\ell+1) \\ & \times \big(\ell(\ell+1) + r^2 f''(r)\big)\Big]\Big[\ell(\ell+1) + rf'(r)\Big] \\ & - f(r)\Big[2\ell(\ell+1) r^2 f''(r) - 2r^4 f''(r)^2 \\ & + \ell(\ell+1)\big(4\ell(\ell+1) + r^3 f'''(r)\big) + rf'(r)\,(2\ell(\ell+1) \\ & + 2r^2 f''(r) + r^3 f'''(r)\big)\Big]\Big\} \end{aligned} \tag{34}$$

for even perturbations (see Appendix A for more details). The above potentials are displayed in Figure 2 for different values of the core radius. One can easily see that the value at the peak of the potential for scalar perturbations decreases for larger cores, whereas it increases for all the other (physically relevant) perturbations, particularly for even gravitational perturbations. The width of the potentials instead increases with the size of the core in all cases. Note that the case $R_{\rm s} = R_{\rm Sch}$ exceeds the bound (18) for the existence of the event horizon and corresponds to a black hole mimicker.

We can compute the quasinormal mode frequencies in the WKB approximation following the procedure proposed in ref. [6]. In a nutshell, one begins by relating the asymptotic expansions at the horizon to the asymptotic expansions at infinity via a Bogoliubov transformation

$$\begin{pmatrix} Z_{\rm H}^{(\rm out)} \\ Z_{\rm H}^{(\rm in)} \end{pmatrix} = \begin{pmatrix} M_{11} & M_{12} \\ M_{21} & M_{22} \end{pmatrix} \begin{pmatrix} Z_{\infty}^{(\rm out)} \\ Z_{\infty}^{(\rm in)} \end{pmatrix}. \tag{35}$$

The element M_{21} turns out to be proportional to $1/\Gamma(-n)$, with n a non-negative integer known as the overtone number expressed by the WKB expansion

$$n + \frac{1}{2} = i\,\frac{(\omega^2 - \bar{V}_j)}{\sqrt{-2\,\bar{V}_j''}} - \Lambda_2 - \Lambda_3 - \Lambda_4 - \dots\,, \tag{36}$$

where Λ_k is a function of n and derivatives of V_j, taken with respect to r_* and evaluated at $r = \bar{r}$ where the potential is maximum, $\bar{V}_j \equiv V_j(\bar{r})$. The boundary conditions (31) imply that $M_{21} = 0$, and Equation (36) then determines the spectrum $\omega = \omega_{n\ell}$ of the quasinormal mode frequencies by relating ω to the overtone number n and the parameters in the potential. The number of terms in each Λ_k grows very fast in size with the expansion, so we will not report here the explicit form of these terms. Further details can be found in ref. [6] for the order up to Λ_3, in ref. [13] for the order up to Λ_6, and in ref. [14] for the order up to Λ_{13}.

The WKB expansion, while providing a very straightforward method for calculating the quasinormal modes frequencies, has some drawbacks. First, the series in Equation (36) is an asymptotic one, so higher-order corrections do not automatically yield more accurate results for ω, and could instead lead to divergences. Moreover, there is no simple way of estimating the error for ω and determine the optimal number of terms to include. Lastly, the method yields sensible results only for small values of the overtone number n, typically for $n \leq \ell$.

Regarding the first issue, it was noted in the literature (see refs. [14, 15]) that one generally obtains better "convergence" properties for ω when Padé approximants are employed.[4] This amounts to replacing the polynomial approximant in Equation (36) with a rational function. In particular, we will use the Padé approximant of order [6/7]. Concerning the error estimate, since we are mostly interested in the order of magnitude of the correction to the standard Schwarzschild values, we will simply not be concerned with it here and restrict our calculation to cases with $n \leq \ell$. In the end, the following computation must be interpreted as a preliminary analysis of ω, since for more

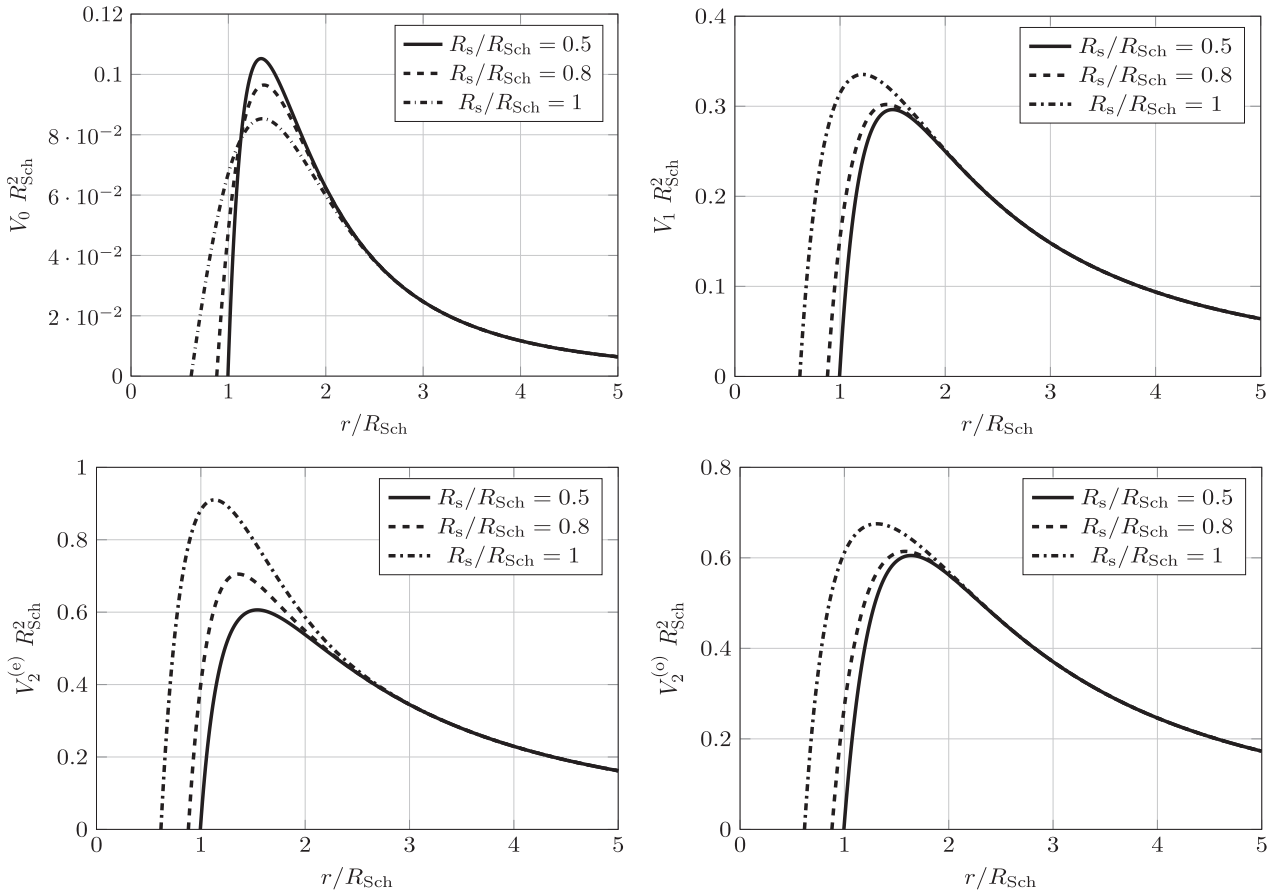

FIGURE 2 | Potentials for the quasinormal modes for different values of R_s: V_0 for scalar perturbations with $\ell = 0$ (top left); V_1 for vector perturbations with $\ell = 1$ (top right); $V_2^{(e)}$ for even tensor perturbations with $\ell = 2$ (bottom left); $V_2^{(o)}$ for odd tensor perturbations with $\ell = 2$ (bottom right).

precise results one would have to employ numerical methods to integrate the differential equations, and cross-reference the results obtained (see, e.g., ref. [18]).

The Mathematica code that implements the calculation of ω, based on the library by Konoplya et al. presented in Ref. [15], as well as the code for the numerical computations in Figure 1, is available upon request from t.antonelli@sussex.ac.uk. The results of the computations obtained with the WKB method are summarised in the following tables, where we present them as the dimensionless quantity ωR_{Sch}. Values of ω in the tables with a question mark (?) indicate cases for which the WKB approximation is not expected to be reliable (see [15] for details).

4 | Discussion and Outlook

In this work, we explored the phenomenology of the quantum-corrected Schwarzschild black hole geometry derived in ref. [2] from the coherent state quantisation of gravity. In particular, we considered constraints on the size R_s of the core for which this geometry represents a black hole, and computed numerically the horizon radius, photon ring, and critical impact parameter. We then compared these observables with those of the classical Schwarzschild geometry.

Following this preliminary investigation of the properties of the proposed geometry, we derived the effective potentials for the Schrödinger-like equations governing scalar, electromagnetic, and gravitational perturbations on this background. In particular, the quasinormal mode frequencies $\omega = \omega_{n\ell}$ for these fields were computed using the standard WKB approximation with appropriate boundary conditions. All throughout the discussion, we set $G = c = 1$ and expressed every quantity in a dimensionless ratio with R_{Sch}; units can be restored by simple considerations of dimensional analysis.

We observe that the quasinormal frequencies in Tables 1–4 deviate only slightly (order of 0.5%) from the Schwarzschild values, for a core of size $R_s = 0.5\, R_{Sch}$. However, the discrepancies become more pronounced for larger values of R_s. In particular, the imaginary part of ω is always smaller than the corresponding Schwarzschild expectation in the computed ranges, and becomes of the order of 5% smaller for $R_s = 0.7\, R_{Sch}$. This result agrees with the behaviour of the width of the potential shown in Figure 2 and indicates that the decay time of such modes become (at least up to about 5%) longer for larger cores, which would affect the duration of ringdown signals during a merger (see, e.g., ref. [19]). The real part of ω, on the contrary, remains relatively unaffected, which means that quasinormal oscillations do not depend significantly on the size of the inner core. Moreover, we show that for values of $R_s \neq 0$, we lose the isospectrality of the even and odd gravitational sectors (Table 5), which is a feature of a classical Schwazschild black hole. Such features could be investigated with the next generation of gravitational wave detectors [20].

TABLE 1 | Scalar field (assuming, for simplicity, $m = 0$).

	Schwarzschild	Quantum ($R_s = 0.5\,R_{Sch}$)	Quantum ($R_s = 0.7\,R_{Sch}$)
$n = 0,\ \ell = 0$	$0.221 - 0.210\,i$ (?)	$0.222 - 0.207\,i$ (?)	$0.218 - 0.184\,i$ (?)
$n = 0,\ \ell = 1$	$0.586 - 0.195\,i$	$0.585 - 0.194\,i$	$0.587 - 0.184\,i$
$n = 1,\ \ell = 1$	$0.529 - 0.612\,i$	$0.527 - 0.612\,i$ (?)	$0.530 - 0.565\,i$ (?)
$n = 0,\ \ell = 2$	$0.967 - 0.194\,i$	$0.967 - 0.193\,i$	$0.969 - 0.183\,i$
$n = 1,\ \ell = 2$	$0.928 - 0.591\,i$	$0.927 - 0.589\,i$	$0.928 - 0.554\,i$
$n = 2,\ \ell = 2$	$0.861 - 1.017\,i$	$0.870 - 1.013\,i$ (?)	$0.865 - 0.948\,i$ (?)
$n = 0,\ \ell = 3$	$1.351 - 0.193\,i$	$1.350 - 0.193\,i$	$1.354 - 0.183\,i$
$n = 1,\ \ell = 3$	$1.321 - 0.585\,i$	$1.320 - 0.583\,i$	$1.323 - 0.552\,i$
$n = 2,\ \ell = 3$	$1.267 - 0.992\,i$	$1.264 - 0.987\,i$	$1.267 - 0.928\,i$
$n = 3,\ \ell = 3$	$1.198 - 1.422\,i$	$1.199 - 1.401\,i$ (?)	$1.212 - 1.316\,i$ (?)

TABLE 2 | Electromagnetic field.

	Schwarzschild	Quantum ($R_s = 0.5\,R_{Sch}$)	Quantum ($R_s = 0.7\,R_{Sch}$)
$n = 0,\ \ell = 1$	$0.497 - 0.185\,i$	$0.497 - 0.184\,i$	$0.502 - 0.173\,i$
$n = 1,\ \ell = 1$	$0.429 - 0.587\,i$	$0.432 - 0.588\,i$ (?)	$0.446 - 0.542\,i$ (?)
$n = 0,\ \ell = 2$	$0.915 - 0.190\,i$	$0.915 - 0.189\,i$	$0.919 - 0.179\,i$
$n = 1,\ \ell = 2$	$0.873 - 0.581\,i$	$0.872 - 0.578\,i$	$0.878 - 0.543\,i$
$n = 2,\ \ell = 2$	$0.802 - 1.003\,i$	$0.802 - 0.993\,i$ (?)	$0.817 - 0.932\,i$ (?)
$n = 0,\ \ell = 3$	$1.314 - 0.191\,i$	$1.313 - 0.191\,i$	$1.318 - 0.181\,i$
$n = 1,\ \ell = 3$	$1.283 - 0.579\,i$	$1.282 - 0.577\,i$	$1.287 - 0.545\,i$
$n = 2,\ \ell = 3$	$1.228 - 0.984\,i$	$1.224 - 0.978\,i$	$1.231 - 0.919\,i$ (?)
$n = 3,\ \ell = 3$	$1.156 - 1.413\,i$	$1.152 - 1.393\,i$ (?)	$1.176 - 1.298\,i$ (?)

TABLE 3 | Gravitational field (odd perturbations).

	Schwarzschild	Quantum ($R_s = 0.5\,R_{Sch}$)	Quantum ($R_s = 0.7\,R_{Sch}$)
$n = 0,\ \ell = 2$	$0.747 - 0.178\,i$	$0.747 - 0.177\,i$	$0.750 - 0.167\,i$
$n = 1,\ \ell = 2$	$0.693 - 0.548\,i$	$0.692 - 0.545\,i$	$0.708 - 0.510\,i$ (?)
$n = 2,\ \ell = 2$	$0.604 - 0.953\,i$ (?)	$0.612 - 0.981\,i$ (?)	$0.636 - 0.897\,i$ (?)
$n = 0,\ \ell = 3$	$1.199 - 0.185\,i$	$1.199 - 0.185\,i$	$1.202 - 0.175\,i$
$n = 1,\ \ell = 3$	$1.165 - 0.563\,i$	$1.164 - 0.560\,i$	$1.169 - 0.529\,i$
$n = 2,\ \ell = 3$	$1.103 - 0.958\,i$	$1.100 - 0.952\,i$	$1.109 - 0.895\,i$ (?)
$n = 3,\ \ell = 3$	$1.024 - 1.381\,i$	$1.030 - 1.358\,i$ (?)	$1.057 - 1.292\,i$ (?)

TABLE 4 | Gravitational field (even perturbations).

	Schwarzschild	Quantum ($R_s = 0.5\,R_{Sch}$)	Quantum ($R_s = 0.7\,R_{Sch}$)
$n = 0,\ \ell = 2$	$0.747 - 0.178\,i$	$0.750 - 0.175\,i$	$0.761 - 0.152\,i$ (?)
$n = 1,\ \ell = 2$	$0.693 - 0.548\,i$	$0.689 - 0.540\,i$ (?)	$0.698 - 0.456\,i$ (?)
$n = 2,\ \ell = 2$	$0.602 - 0.956\,i$ (?)	$0.571 - 0.957\,i$ (?)	$0.539 - 0.721\,i$ (?)
$n = 0,\ \ell = 3$	$1.199 - 0.185\,i$	$1.200 - 0.183\,i$	$1.218 - 0.172\,i$
$n = 1,\ \ell = 3$	$1.165 - 0.563\,i$	$1.167 - 0.557\,i$	$1.192 - 0.521\,i$ (?)
$n = 2,\ \ell = 3$	$1.103 - 0.958\,i$	$1.106 - 0.952\,i$ (?)	$1.149 - 0.895\,i$ (?)
$n = 3,\ \ell = 3$	$1.024 - 1.381\,i$	$1.037 - 1.401\,i$ (?)	$1.085 - 1.338\,i$ (?)

TABLE 5 | Deviation of the real and imaginary part between even and odd gravitational QNMs.

	$(\mathbf{Re}(\omega_o) - \mathbf{Re}(\omega_e))/\mathbf{Re}(\omega_o)$		$(\mathbf{Im}(\omega_o) - \mathbf{Im}(\omega_e))/\mathbf{Im}(\omega_o)$	
	$R_s = 0.5\,R_{Sch}$	$R_s = 0.7\,R_{Sch}$	$R_s = 0.5\,R_{Sch}$	$R_s = 0.7\,R_{Sch}$
$n = 0,\ \ell = 2$	−0.004	−0.015	0.011	0.087
$n = 1,\ \ell = 2$	0.005	0.013	0.009	0.106
$n = 2,\ \ell = 2$	0.068	0.152	0.025	0.197
$n = 0,\ \ell = 3$	−0.001	−0.013	0.007	0.017
$n = 1,\ \ell = 3$	−0.003	−0.022	0.006	0.014
$n = 2,\ \ell = 3$	−0.005	−0.036	0.000	0.000
$n = 3,\ \ell = 3$	−0.007	−0.026	−0.032	−0.036

We expect even larger deviations for larger values of R_s. However, the WKB method begins to show its limits in this regime. At $R_s = 0.7\,R_{Sch}$, the WKB expansion turns out to be unreliable for many modes, especially in the gravitational sector. Moreover, we recall that the horizon exists only for inner cores of size $R_s \lesssim 0.84\,R_{Sch}$. Larger cores correspond to black hole mimickers without an event horizon, for which the existence of quasinormal oscillations will strongly depend on the boundary condition at the surface $r = R_s$ (which we have not analysed here). Thus, our analysis of the quasinormal frequencies can serve as a *preliminary estimate* of the order of magnitude of deviations of this quantum-corrected geometry from the classical case. More refined results would require fully numerical calculations, which is, however, beyond the scope of this work.

Acknowledgements

The work of T.A. is supported by a doctoral studentship of the Science and Technology Facilities Council (training grant No. ST/Y509620/1, project ref. 2917813). A.G. is supported by the Italian Ministry of Universities and Research (MUR) through the grant "BACHQ: Black Holes and The Quantum" (grant no. J33C24003220006). A.G. and R.C. carried out this work in the framework of the activities of the Italian National Group of Mathematical Physics [Gruppo Nazionale per la Fisica Matematica (GNFM), Istituto Nazionale di Alta Matematica (INdAM)]. R.C. and A.G. are partially supported by the INFN grant FLAG.

Open access publishing facilitated by Universita di Bologna, as part of the Wiley - CRUI-CARE agreement.

Funding

T.A. is supported by a doctoral studentship of the Science and Technology Facilities Council (training grant No. ST/Y509620/1, project ref. 2917813). A.G. is supported by the Italian Ministry of Universities and Research (MUR) through the grant "BACHQ: Black Holes and The Quantum" (grant no. J33C24003220006).

Conflicts of Interest

The authors declare no competing interests.

Data Availability Statement

This is a purely theoretical study; no new data were created or analysed in this research.

The Mathematica code implementing the calculations in this work is based on the library by Konoplya et al. [15]. The code used for the numerical computations is available upon reasonable request at t.antonelli@sussex.ac.uk.

Endnotes

[1] For the sake of convenience, we set Newton's gravitational constant and the reduced Planck constant to unity.

[2] These modes decouple in the static and spherically symmetric background (1).

[3] This strictly classical property of the horizon is further analysed in the quantum theory in ref. [2].

[4] Notably, Padé approximants have important applications beyond black hole perturbation theory; for example, they also play a significant role in cosmology (see, e.g., [16, 17])

[5] As a point of clarity, to fully reconstruct the metric perturbations, one would need to also consider the perturbation to the matter equations of motion, which are not known to us. This is a limitation in our approach, hence we will only focus on the perturbed Einstein's equations, from which we will be able to reconstruct the generalised form of the Regge–Wheeler and Zerilli potentials for this geometry.

[6] Physically, ϵ represents matter modes that are not fixed by the metric modes. In the case of odd gravitational perturbations it turns out that the metric and matter modes do not couple, so we may as well set ϵ to zero for the purposes of our analysis. This will change for the even sector, where in that case we will need to use our gauge freedom to decouple the two modes.

References

1. R. Casadio, "Geometry and Thermodynamics of Coherent Quantum Black Holes," *International Journal of Modern Physics A D* 31 (2022): 2250128, https://doi.org/10.1142/S0218271822501280.

2. W. Feng, A. Giusti, and R. Casadio, "Horizon Quantum Mechanics for Coherent Quantum Black Holes," *European Physical Journal Plus* 140 (2025): 145, https://doi.org/10.1140/epjp/s13360-025-06065-x.

3. R. Casadio, A. Giusti, and J. Ovalle, "Quantum Reissner-Nordström Geometry: Singularity and Cauchy Horizon," *Physical Review D* 105 (2022): 124026, https://doi.org/10.1103/PhysRevD.105.124026.

4. E. Berti, V. Cardoso, and A. O. Starinets, "Quasinormal Modes of Black Holes and Black Branes," *Classical and Quantum Gravity* 26 (2009): 163001, https://doi.org/10.1088/0264-9381/26/16/163001.

5. K. D. Kokkotas and B. G. Schmidt, "Quasinormal modes of stars and black holes," *Living Reviews in Relativity* 2 (1999): 2, https://doi.org/10.12942/lrr-1999-2.

6. S. Iyer and C. M. Will, "Black Hole Normal Modes: A WKB Approach. 1. Foundations and Application of a Higher Order WKB Analysis of Potential-Barrier Scattering," *Physical Review D* 35 (1987): 3621, https://doi.org/10.1103/PhysRevD.35.3621.

7. V. Faraoni, *Cosmological and Black Hole Apparent Horizons* (Springer, 2015), https://doi.org/10.1007/978-3-319-19240-6.

8. R. Casadio, A. Giusti, and J. Ovalle, "Quantum Rotating Black Holes," *Journal of High Energy Physics* 05 (2023): 118, https://doi.org/10.1007/JHEP05(2023)118.

9. V. N. Lukash and V. N. Strokov, "Space-Times With Integrable Singularity," *International Journal of Modern Physics A* 28 (2013): 1350007, https://doi.org/10.1142/S0217751X13500073.

10. P. O. Mazur and E. Mottola, "Gravitational Vacuum Condensate Stars," *Proceedings of the National Academy of Sciences* 101 (2004): 9545–9550, https://doi.org/10.1073/pnas.0402717101.

11. A. Urmanov, H. Chakrabarty, and D. Malafarina, "Observational Properties of Coherent Quantum Black Holes," *Physical Review D* 110 (2024): 044030, https://doi.org/10.1103/PhysRevD.110.044030.

12. L. C. B. Crispino, A. Higuchi, and G. E. A. Matsas, "Quantization of the Electromagnetic Field Outside Static Black Holes and Its Application to Low-Energy Phenomena," *Physical Review D* 63 (2001): 124008, https://doi.org/10.1103/PhysRevD.80.029906. [Erratum: Phys. Rev. D 80 (2009): 029906].

13. R. A. Konoplya, "Quasinormal Behavior of the D-Dimensional Schwarzschild Black Hole and Higher Order WKB Approach," *Physical Review D* 68 (2003): 024018, https://doi.org/10.1103/PhysRevD.68.024018.

14. J. Matyjasek and M. Opala, "Quasinormal Modes of Black Holes. The Improved Semianalytic Approach," *Physical Review D* 96 (2017): 024011, https://doi.org/10.1103/PhysRevD.96.024011.

15. R. A. Konoplya, A. Zhidenko, and A. F. Zinhailo, "Higher Order WKB Formula for Quasinormal Modes and Grey-Body Factors: Recipes for Quick and Accurate Calculations," *Classical and Quantum Gravity* 36 (2019): 155002, https://doi.org/10.1088/1361-6382/ab2e25.

16. C. Gruber and O. Luongo, "Cosmographic Analysis of the Equation of State of the Universe Through Padé Approximations," *Physical Review D* 89, no. 10, (2014): 103506, https://doi.org/10.1103/PhysRevD.89.103506, `arXiv:1309.3215 [gr-qc]`.

17. A. Aviles, A. Bravetti, S. Capozziello, and O. Luongo, "Precision Cosmology With Padé Rational Approximations: Theoretical Predictions Versus Observational Limits," *Physical Review D* 90, no. 4 (2014): 043531, `arXiv:1405.6935 [gr-qc]`.

18. R. A. Konoplya, A. F. Zinhailo, J. Kunz, Z. Stuchlik, and A. Zhidenko, "Quasinormal Ringing of Regular Black Holes in Asymptotically Safe Gravity: The Importance of Overtones," *Journal of Cosmology and Astroparticle Physics* 10 (2022): 091, https://doi.org/10.1088/1475-7516/2022/10/091.

19. F. Nobili, S. Bhagwat, C. Pacilio, and D. Gerosa, "Ringdown Mode Amplitudes of Precessing Binary Black Holes," *Physical Review D* 112, no. 4 (2025): 044058, https://doi.org/10.1103/cl3k-3xt2.

20. A. Abac, R. Abramo, S. Albanesi, et al., "The Science of the Einstein Telescope," http://arxiv.org/abs/2503.12263.

21. T. Regge and J. A. Wheeler, "Stability of a Schwarzschild Singularity," *Physical Review D* 108 (1957): 1063–1069, https://doi.org/10.1103/PhysRev.108.1063.

22. V. Moncrief, "Gravitational Perturbations of Spherically Symmetric Systems. I. The Exterior Problem," *Annals of Physics* 88 (1974): 323–342, https://doi.org/10.1016/0003-4916(74)90173-0.

23. F. J. Zerilli, "Effective Potential for Even Parity Regge-Wheeler Gravitational Perturbation Equations," *Physical Review Letters* 24 (1970): 737–738, https://doi.org/10.1103/PhysRevLett.24.737.

Appendix A: Quasinormal Modes Potentials for the Gravitational Sector

Scalar, electromagnetic and gravitational perturbations on the background metric (1) decouple, since the coupling between different perturbations is proportional to the stress–energy tensor of the background solution, which is assumed to be generated by some other unspecified field.

Compared to the scalar and electromagnetic fields, the gravitational perturbations are more involved, the main technical difficulty being the fact that the background has a non-vanishing stress–energy tensor which interacts non-trivially with the gravitational perturbations. We start from the decomposition of the metric into background, given in Equation (1), and perturbations,

$$g_{\mu\nu} = \bar{g}_{\mu\nu} + h_{\mu\nu}\,, \tag{A1}$$

which yields the perturbations of the Einstein equations

$$\frac{\delta}{\delta g_{\rho\sigma}}(G^{\mu\nu} - 8\,\pi\,T^{\mu\nu})\bigg|_{\bar{g}} h_{\rho\sigma} = 0\,. \tag{A2}$$

In the (t, r, θ, φ) coordinates of the background, the gravitational perturbation under spatial rotations $SO(3)$ transforms as

$$h_{\mu\nu} = \begin{pmatrix} \boxed{\text{S}} & \boxed{\text{S}} & \boxed{\text{V}} \\ \boxed{\text{S}} & \boxed{\text{S}} & \boxed{\text{V}} \\ \boxed{\text{V}} & \boxed{\text{V}} & \boxed{\text{T}} \end{pmatrix} \tag{A3}$$

where S, V and T denote a scalar, vector and tensor behaviour, respectively. We thus can introduce the vector spherical harmonics

$$Y^{(1)}_{\ell m,\,a}(\theta,\varphi) = \left(\partial_\theta Y_{\ell m}\,,\, \partial_\varphi Y_{\ell m}\right) \tag{A4}$$

$$Y^{(2)}_{\ell m,\,a}(\theta,\varphi) = \left(\frac{1}{\sin\theta}\,\partial_\varphi Y_{\ell m}\,,\, -\sin\theta\,\partial_\theta Y_{\ell m}\right) \tag{A5}$$

and the tensor spherical harmonics

$$Y^{(1)}_{\ell m,\,ab}(\theta,\varphi) = \begin{pmatrix} \partial^2_\theta\, Y_{\ell m} & (\partial_\theta - \cot\theta)\partial_\varphi Y_{\ell m} \\ * & (\partial^2_\varphi + \sin\theta\cos\theta\,\partial_\theta) Y_{\ell m} \end{pmatrix} \tag{A6}$$

$$Y^{(2)}_{\ell m,\,ab}(\theta,\varphi) = \begin{pmatrix} Y_{\ell m} & 0 \\ * & \sin^2\theta\, Y_{\ell m} \end{pmatrix} \tag{A7}$$

$$Y^{(3)}_{\ell m,\,ab}(\theta,\varphi) = \begin{pmatrix} \frac{1}{\sin\theta}(\partial_\theta - \cot\theta)\partial_\varphi Y_{\ell m} & \frac{1}{2}\left(\frac{1}{\sin\theta}\partial^2_\varphi + \cos\theta\,\partial_\theta - \sin\theta\,\partial^2_\theta\right) Y_{\ell m} \\ * & -\sin\theta(\partial_\theta - \cot\theta)\partial_\varphi Y_{\ell m} \end{pmatrix}. \tag{A8}$$

The perturbation $h_{\mu\nu}$ correspondingly decomposes into even and odd parts under parity,

$$h^{(e)}_{\mu\nu}(t,r,\theta,\varphi)$$

$$= e^{-i\omega t}\begin{pmatrix} f(r)H_0(r)Y_{\ell m} & i\omega H_1(r)Y_{\ell m} & i\omega F_0(r)\,Y^{(1)}_{\ell m,a} \\ * & \frac{1}{f(r)}H_2(r)Y_{\ell m} & F_1(r)\,Y^{(1)}_{\ell m,a} \\ * & * & r^2\left(G(r)Y^{(1)}_{\ell m,ab}+K(r)Y^{(2)}_{\ell m,ab}\right)\end{pmatrix} \tag{A9}$$

$$h^{(o)}_{\mu\nu}(t,r,\theta,\varphi) = e^{-i\omega t}\begin{pmatrix} 0 & 0 & i\omega\, h_0(r)\,Y^{(2)}_{\ell m,a} \\ * & 0 & h_1(r)\,Y^{(2)}_{\ell m,a} \\ * & * & r^2\,h_2(r)\,Y^{(3)}_{\ell m,ab}\end{pmatrix}. \tag{A10}$$

Now, the perturbation of the Einstein tensor is readily obtained

$$\left.\frac{\delta G_{\mu\nu}}{\delta g_{\rho\sigma}}\right|_{\bar g} h_{\rho\sigma} = \frac{1}{2}\Big(\bar\nabla_\rho\bar\nabla_\mu h_\nu{}^\rho + \bar\nabla_\rho\bar\nabla_\nu h_\mu{}^\rho - \bar\nabla_\mu\bar\nabla_\nu h_\rho{}^\rho - \bar\nabla_\rho\bar\nabla^\rho h_{\mu\nu}$$
$$- \bar R h_{\mu\nu} + \bar g_{\mu\nu}\bar\nabla_\rho\bar\nabla^\rho h_\sigma{}^\sigma - \bar g_{\mu\nu}\bar\nabla_\rho\bar\nabla_\sigma h^{\rho\sigma} + \bar g_{\mu\nu}\bar R_{\rho\sigma}h^{\rho\sigma}\Big)\,. \tag{A11}$$

For the stress–energy tensor, which has a background value of

$$\bar T_{\mu\nu} = \bar\rho\,\bar u_\mu\,\bar u_\nu + \bar p_r\,\bar r_\mu\,\bar r_\nu + \bar p_\varphi\big(\bar g_{\mu\nu} + \bar u_\mu\,\bar u_\nu - \bar r_\mu\,\bar r_\nu\big)\,, \tag{A12}$$

where

$$\bar u_\mu = \Big(-\sqrt{f(r)},\,0,\,0,\,0\Big),\quad \bar r_\mu = \Big(0,\,1/\sqrt{f(r)},\,0,\,0\Big),$$
$$\bar\rho = -\bar p_r = \frac{1-f(r)-r\,f'(r)}{r^2},\quad \bar p_\varphi = \frac{2f'(r)+r\,f''(r)}{2r}\,, \tag{A13}$$

the dependence on the metric is implicit, so one can calculate the perturbations on general grounds by imposing the variation

$$u_\mu = \bar u_\mu + \delta u_\mu,\quad r_\mu = \bar r_\mu + \delta r_\mu,$$
$$\rho = \bar\rho + \delta\rho,\quad p_r = \bar p_r + \delta p_r,\quad p_\varphi = \bar p_\varphi + \delta p_\varphi\,, \tag{A14}$$

where the perturbations δu_μ and δr_μ can be fixed via the perturbed orthonormality conditions

$$\delta u_\mu\,\bar u^\mu = \frac{h^{\mu\nu}\bar u_\mu\bar u_\nu}{2},\quad \delta r_\mu\,\bar r^\mu = \frac{h^{\mu\nu}\bar r_\mu\bar r_\nu}{2},\quad \delta u_\mu\,\bar r^\mu + \delta r_\mu\,\bar u^\mu = h^{\mu\nu}\bar u_\mu\bar r_\nu\,, \tag{A15}$$

and $\delta\rho, \delta p_r$ and δp_φ can be fixed via the perturbed conservation equation

$$\bar\nabla^\mu\left(\left.\frac{\delta T_{\mu\nu}}{\delta g_{\rho\sigma}}\right|_{\bar g} h_{\rho\sigma}\right) = \bar\nabla^\mu\big(h_\mu{}^\rho\,\bar T_{\rho\nu}\big) + \frac{1}{2}\bar\nabla_\nu(h^{\rho\sigma})\bar T_{\rho\sigma} - \frac{1}{2}\bar\nabla^\mu\big(h_\rho{}^\rho\big)\bar T_{\mu\nu}\,. \tag{A16}$$

Explicitly, since we do not know the functional dependence on the metric of this effective stress–energy tensor, we employed an effective description of this object, and treated it as an anisotropic fluid subject to perturbations. In this formalism, strictly speaking, we are not just perturbing the metric degrees of freedom, but also the (unknown) matter degrees of freedom that generate the background metric, since a priori the two are coupled to each other. In the following, we will show how these additional matter degrees of freedom show up and how to decouple them from the gravitational perturbations.[5]

Given the previous conditions in Equations (A15) and (A16), we obtain a physically sensible perturbation of the stress–energy tensor, which takes then the following form:

$$\left.\frac{\delta T_{\mu\nu}}{\delta g_{\rho\sigma}}\right|_{\bar g} h_{\rho\sigma} = \delta\rho\,\bar u_\mu\,\bar u_\nu + \delta p_r\,\bar r_\mu\,\bar r_\nu + \delta p_\varphi\big(\bar g_{\mu\nu} + \bar u_\mu\,\bar u_\nu - \bar r_\mu\,\bar r_\nu\big)$$
$$+ 2\,\bar\rho\,\delta u_{(\mu}\,\bar u_{\nu)} + 2\,\bar p_r\,\delta r_{(\mu}\,\bar r_{\nu)}$$
$$+ \bar p_\varphi\big(h_{\mu\nu} + 2\,\delta u_{(\mu}\,\bar u_{\nu)} - 2\,\delta r_{(\mu}\,\bar r_{\nu)}\big). \tag{A17}$$

Now, for the study of the odd gravitational perturbations, which are algebraically simpler, we impose the Regge–Wheeler gauge [21] and set $h_2 = 0$ in (A10). From (A15), we get

$$\delta u^{(o)}_\mu = \delta r^{(o)}_\mu = 0\,, \tag{A18}$$

while from Equation (A16) we get

$$\delta\rho^{(o)} = \delta p^{(o)}_\varphi = 0 \tag{A19}$$

$$\delta p^{(o)}_r = e^{-i\omega t}\,Y_{\ell m}\,\frac{\epsilon}{\sqrt{f(r)}r^2}\,, \tag{A20}$$

where ϵ is an arbitrary constant of integration that comes out of the conservation equation, which by consistency must be in the order of the perturbations.[6] After writing down the explicit form of the perturbed Einstein equations and relabelling

$$\psi^{(o)}_2 = \frac{f(r)\,h_1}{r}\,, \tag{A21}$$

we get the Schrödinger-like equation (27) with the potential in Equation (33).

For the even gravitational perturbations, the gauge choice is not as simple anymore. We will fix $F_0 = 0$, while F_1 and G will be implicitly defined such as to satisfy the following equations:

$$G = \frac{4f(r)}{\ell(\ell+1)rf'(r)}$$
$$\times\left[\ell(\ell+1)\left(\frac{F_1}{r} - \frac{r}{2}\frac{dG}{dr}\right) + H_0 - H_2 + r\frac{dK}{dr} + \frac{rf'(r)}{2f(r)}K\right] \tag{A22}$$

$$F_1 = \frac{rK}{2f(r)} - \frac{\tilde\epsilon\,r}{f(r)^{3/2}\,(2-2f(r)+r^2f''(r))}$$
$$+ \frac{rG}{4f(r)(\ell(\ell+1)-2f(r)+rf'(r))(2-2f(r)+r^2f''(r))}$$
$$\times\Big\{\big[2+r^2f''(r)\big]\big[(\ell(\ell+1))^2 - \ell(\ell+1)rf'(r) - 2r^2f'(r)^2\big]$$
$$+ 4f(r)^2\big[\ell(\ell+1) - 2rf'(r) + r^3f'''(r)\big]$$
$$- 2f(r)\big[-4r^2f'(r)^2 + (-4+3\ell(\ell+1))\,r^2f''(r)$$
$$- 2r^4f''(r)^2 + \ell(\ell+1)(\ell(\ell+1)+2+r^3f'''(r))$$
$$+ rf'(r)(-3\ell(\ell+1)+2r^2f''(r)+r^3f'''(r))\big]\Big\}\,, \tag{A23}$$

where $\tilde\epsilon$ is an arbitrary constant for now. As we did for the odd perturbations, we can now calculate δu_μ, δr_μ, $\delta\rho$, δp_r and δp_ϕ with this specific form of the perturbation. A short calculation with Equation (A15) reveals that

$$\delta u^{(e)}_\mu = e^{-i\omega t}\,Y_{\ell m}\left(\frac{\sqrt{f(r)}\,H_0}{2},\,\frac{H_1}{2\sqrt{f(r)}},\,0,\,0\right) \tag{A24}$$

$$\delta r_{\mu}^{(\mathrm{e})} = e^{-i\omega t}\, Y_{\ell m}\left(\frac{\sqrt{f(r)}H_1}{2},\ \frac{H_2}{2\sqrt{f(r)}},\ 0,\ 0\right), \tag{A25}$$

while from (A16) we get that

$$\delta p_{\varphi}^{(\mathrm{e})} = e^{-i\omega t}\, Y_{\ell m}\, \frac{2 - 2f(r) + r^2 f''(r)}{2r^3}(H_0 - H_2) \tag{A26}$$

$$\delta \rho^{(\mathrm{e})} = e^{-i\omega t}\, Y_{\ell m}\, \frac{2 - 2f(r) + r^2 f''(r)}{2r^2}\left[\frac{\ell(\ell+1)}{2}G - K\right] \tag{A27}$$

$$\delta p_{r}^{(\mathrm{e})} = e^{-i\omega t}\, Y_{\ell m}\, \frac{\epsilon}{\sqrt{f(r)}r^2}, \tag{A28}$$

where again ϵ is a constant of integration in the order of the perturbations. This result is highly non-trivial, because now, for the even perturbations, the conservation equation (A16) prescribes a rather involved differential equation for δp_r, where the matter degrees of freedom get mixed with the gravitational perturbations ones. The gauge choice for G in Equation (A22) has the precise effect of decoupling the two different degrees of freedom and producing an integrable differential equation for δp_r, which results in the simple form in Equation (A28). Since for the previous calculations the value of $\tilde{\epsilon}$ in Equation (A23) was irrelevant, we may fix it now to be $\tilde{\epsilon} = \epsilon$.

The process of extracting now the Schrödinger-like equation from the perturbed Einstein equations is straightforward, even though tedious. Motivated by [22], we introduce the relabelling

$$\psi_2^{(\mathrm{e})} = r\,K + \frac{2f(r)}{\ell(\ell+1) - 2f(r) + r f'(r)} \times \left[rH_2 - r^2\frac{dK}{dr} + \ell(\ell+1)\left(\frac{r^2}{2}\frac{dG}{dr} - F_1\right)\right], \tag{A29}$$

which is the variable that will appear in Equation (27). One eventually arrives at the potential given in Equation (34), with the gauge condition (A23) playing a crucial role for simplifying the final expression. The potential in Equation (34) is the generalisation in our context of the Zerilli potential for a Schwarzschild black hole [22, 23].